Advanced Techniques for Frequency Estimation from LDA Burst Signals

Holger Nobach

Dantec Measurement Technology, Tonsbakken 16–18, DK-2740 Skovlunde, Denmark
holger.nobach@dantecmt.com

One of the most important quantities in burst signals from LDA measurements is the Doppler frequency which corresponds to the velocity of the detected particle. This article describes new algorithms for estimating the Doppler frequency from LDA burst signals with very small statistical fluctuations using model-based or parametric procedures. The results are compared to the three-point Gauss interpolation from the power spectral density.

1. INTRODUCTION

The most important parameter of a burst signal recorded by a laser Doppler anemometer is the Doppler frequency. The frequency estimate leads to the velocity of the detected tracer particle but has some principle limits in it's accuracy [1] which appears as random noise in the velocity series. Minimizing this noise is very important e.g. for the estimation of turbulence spectra. A smaller noise level increases the range of correct spectral estimates up to higher frequencies and to lower power spectral densities.

Generally, frequency domain processing using the power spectral density (PSD) [2, 4, 7] or the autocorrelation function (ACF) [3] are superior to time domain estimation of the Doppler frequency, however usually stationarity over the obseration time is assumed. The variance of an ideal estimator, i.e. with the minimum estimation variability is given by the Cramer-Rao-Lower-Bound (CRLB) [6, 8].

An improvement to established parameter estimation procedures can be obtained by using model-based estimation, as outlined for instance in [5]. With this technique the signal character must be known beforehand and the model parameters are chosen to achieve a best fit to the signal.

An appropriate model of an LDA burst (with DC part removed) is the Gauss modulated cosine function

$$u(t) = A_t G\left(\frac{t-t_0}{b_t}\right)\cos(2\pi t f_D + \phi) \tag{1}$$

with the Gauss-like function $G(x) = e^{-x^2/2}$, the signal amplitude A_t, the Doppler frequency f_D, the phase ϕ, the arrival time t_0 and the width b_t of the Gauss envelope given through the size of the measurement volume. The ACF of such a signal is

$$R(\tau) = A_R G\left(\frac{\tau}{b_R}\right)\cos(2\pi\tau f_D) \tag{2}$$

with $b_R = \sqrt{2}b_t$ and the PSD is

$$S(f) = A_S\left[G\left(\frac{f-f_D}{b_S}\right) + G\left(\frac{f+f_D}{b_S}\right)\right] \tag{3}$$

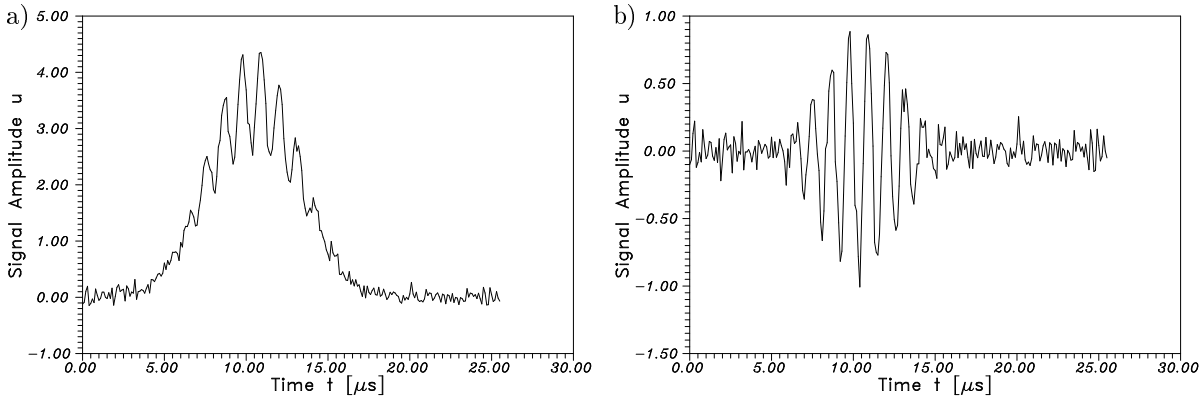

Figure 1: Simulated burst signal a) with DC part and b) filtered.

with $b_S = \frac{1}{2\pi b_R}$.

Therefore, the best model to estimate the Doppler frequency is the Gauss function for the estimation based on the PSD and the Gauss modulated cosine function for the ACF based estimation.

In the following section the procedures of burst signal processing are introduced in detail. The performance of the new estimators has been investigated using numerical simulations that are described in section 3.. The results of that performance test are presented in section 4.. The last section discusses the results and derives some tasks for future work.

2. SIGNAL PROCESSING

2.1 Filter

To split the burst signal (figure 1a) into its AC and DC part a digital filter based on discrete Fourier transfom (DFT) is used. The equidistant sampled time signal u_i is transformed into the frequency domain using the DFT

$$U_j = \sum_{i=0}^{N-1} u_i e^{-2\pi \mathrm{i} ij/N} \qquad j = 0 \ \ldots \ N-1 \tag{4}$$

with the imaginary unit i and the complex amplitude spectrum U_j of the burst signal. Note that the spectrum is symmetric to $J = N/2$. To suppress the DC part of the burst signal all spectral values with corresponding frequencies $f_j = f_s j/N$ which are smaller than a given cut-off frequency $f_c = 0.4\,\mathrm{MHz}$ are set to zero, that means for all $j < Nf_c/f_s$. With respect to the symmetry, the same has to be done for all $j > N(1 - f_c/f_s)$. The new complex amplitude spectrum is transformed back to the time domain using the inverse DFT (IDFT).

$$u_i = \frac{1}{N} \sum_{j=0}^{N-1} U_j e^{2\pi \mathrm{i} ij/N} \qquad i = 0 \ \ldots \ N-1 \tag{5}$$

Since the spectrum remains symmetry about zero (even function), also the filtered time signal is real. The phase information in the high frequency range is preserved through this procedure. Figure 1b shows the filtered signal of the burst shown in figure 1a.

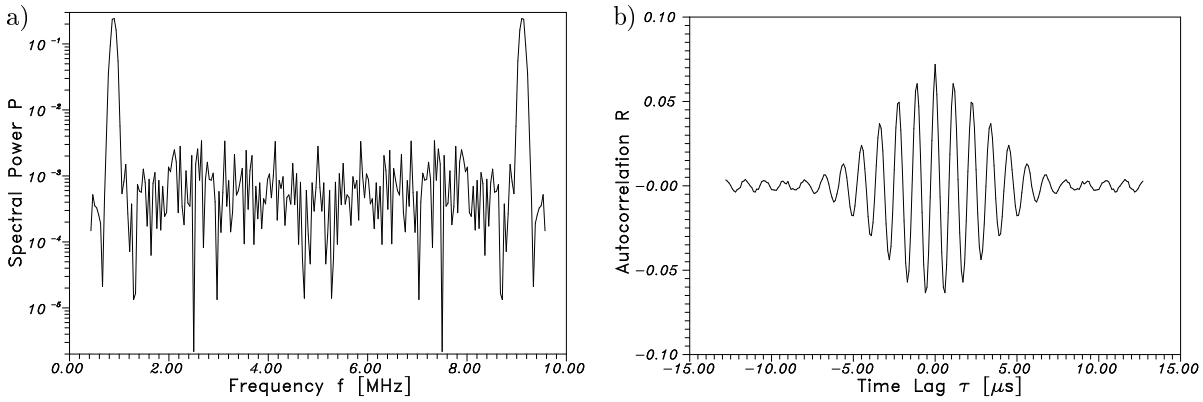

Figure 2: a) Power spectrum and b) autocorrelation function of a burst signal

2.2 Signal-To-Noise-Ratio

The signal-to-noise-ratio (SNR) of the input signal is taken from the filtered signal. It is defined as

$$\mathrm{SNR/dB} = 10 \log_{10} \left(\frac{\sigma_S^2}{\sigma_N^2} \right) \tag{6}$$

with the signal power (variance) σ_S^2 and the noise power (variance) σ_N^2. To calculate this value a separation of the signal and the noise is required. In real measurements the noise free signal is not accessable. For this reason several definitions exist using various assumptions about the signal characteristics. In this paper only numerical simulations will be used. Therefore, a noise free signal can be generated where the noise is added in a second step. Therefore, the definition given by equation (6) can be used directly. All calculations (signal generating and filtering) have to be performed once with the noise free signal to obtain a reference and a second time with the added noise.

2.3 Statistical Functions

The next step of the signal processing is the calculation of statistical functions. This requires that all parameters of the signal are constant within the recorded time. Especially, the Doppler frequency has to be time independent. In that case, the ACF and the PSD contain all signal quantities except the information about arrival time or the spectral phase. The frequency estimation can be performed on these functions much better than from the original time signal because of the better separation of noise and signal components.

The PSD of the simulated (and filtered) burst signal can be calculated using

$$S_j = \frac{1}{f_s N} \left| \sum_{i=0}^{N-1} u_i e^{-2\pi \mathbb{i} i j / N} \right|^2 \qquad j = 0 \ \ldots \ N-1. \tag{7}$$

Figure 2a shows the PSD of the burst shown in figure 1.

The autocorrelation function of the simulated (and filtered) burst signal can be calculated using

$$R_i = \frac{f_s}{N} \sum_{j=0}^{N-1} S_j e^{2\pi \mathbb{i} i j / N} \qquad i = -\frac{N}{2} \ \ldots \ \frac{N}{2} - 1. \tag{8}$$

Figure 2b shows the ACF of the burst shown in figure 1. The noise peak at $\tau = 0$ is small but evident.

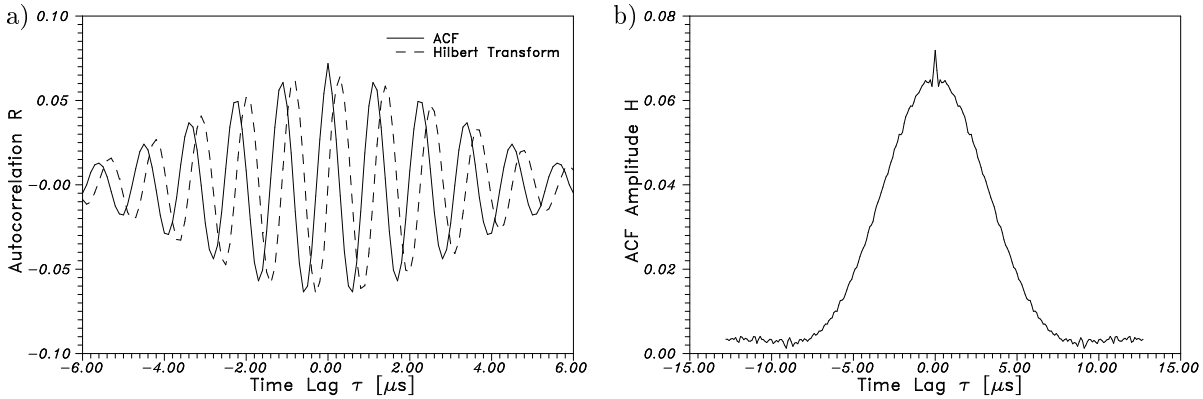

Figure 3: a) The ACF and the corresponding Hilbert transform and b) the ACF amplitude function

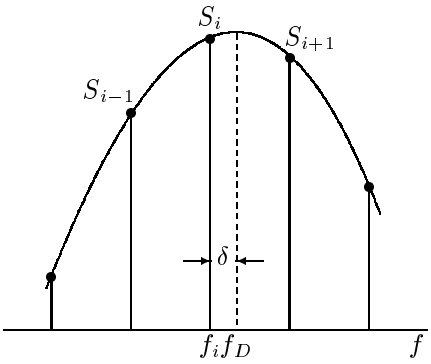

Figure 4: Spectral peak interpolation scheme

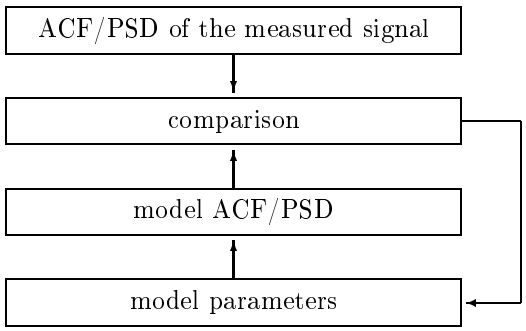

Figure 5: A schematic representation of model parameter estimation

One proposed frequency estimator uses the envelope of the modulated cosine in the ACF. To obtain the envelope the Hilbert transform can be used. The Hilbert transform of a given signal can be calculated as follows. The Fourier transform (equation 4) is performed on the signal and the complex spectral amplitude is obtained. The spectral coefficient are inverted for $j \geq N/2$. An inverse Fourier transform (equation 5) then of this asymmetric spectrum leads to a complex signal with the Hilbert transform in the imaginary part. Figure 3a shows the ACF R_i and the corresponding Hilbert transform R_{Hi}. The ACF amplitude function can be obtained as

$$H_i = \sqrt{R_i^2 + R_{Hi}^2} \tag{9}$$

Figure 3b shows the ACF amplitude function of the burst shown in figure 1. The noise peak at $\tau = 0$ can also be seen here very clearly.

2.4 Frequency Estimation

2.4.1 Three-Point Gauss Interpolation

To evaluate the performance of the new frequency estimators a comparison to the three-point Gauss interpolation [2] was realized. The algorithm includes the maximum of the PSD and the two neighbouring values. The use of a logarithmic scaling reduces the Gauss function to a second order polynomial. Assuming, S_i is the maximum spectral value and S_{i-1} and S_{i+1} are the values of the preceding and the following spectral lines, the deviation δ of the refined Doppler frequency

estimate to the index i of the maximum spectral value (figure 4) becomes

$$\delta = \frac{s_{i-1} - s_{i+1}}{2(s_{i+1} - 2s_i + s_{i-1})} \tag{10}$$

with the notation $s_j = \log_e S_j$. The Doppler frequency becomes

$$f_D = (i + \delta) f_s / N. \tag{11}$$

2.4.2 All Points Gauss Fit

A more accurate algorithm can be obtained by fitting the entire PSD by a Gauss function. The solution cannot fit all spectral points and has to be done model-based [5]. The basic procedure to be followed is shown schematically in figure 5. The estimated PSD S_j is compared to the model PSD

$$S_j^{(m)} = A_S G\left(\frac{f_j - f_D}{b_S}\right) \qquad j = 0 \ \ldots \ N/2 \tag{12}$$

with $f_j = f_s j / N$ and the three parameters A_S, f_D and b_S. The upper index (m) indicates the *model* PSD in contrast to the PSD of the measured or simulated signal (without an upper index).

The deviation between the two functions are evaluated as an error value

$$e = \sum_{j=\lfloor N f_c / f_s \rfloor + 1}^{N/2} \left(S_j - S_j^{(m)}\right)^2, \tag{13}$$

which is used to alter the model parameters to achieve the minimum deviation iteratively. The resultant parameter set then represents the best match of the model to the PSD of the measured burst signal.

The optimum amplitude A_S in equation (12) can be expressed explicitly by

$$A_S = \frac{\sum_{j=\lfloor N f_c / f_s \rfloor + 1}^{N/2} S_j G\left(\frac{f_j - f_D}{b_S}\right)}{\sum_{j=\lfloor N f_c / f_s \rfloor + 1}^{N/2} \left(G\left(\frac{f_j - f_D}{b_S}\right)\right)^2}. \tag{14}$$

To find the optimum of the remaining parameters a searching routine is used that optimizes the parameter set recursively. It starts with the initial parameter set $b_S = f_D = f_s/4$. Both parameters are then varied randomly with a Gauss distribution and a standard deviation of $f_s/4$. If a better parameter set with a smaller error e is found, this parameter set becomes the center of further iterations. The frequency range for f_D should be limited to the range between the cut-off frequency f_c of the high pass filter (section 2.1) and half of the Fourier frequency range $f_s/2$. The Gauss width b_S should be positive. To reduce the searching range and to obtain convergence, the standard deviation of the Gauss distribution has to be reduced from iteration step to iteration step by a constant factor. The factor has been chosen in such a way that after 20 000 steps a distribution width of 1×10^{-6} MHz has been reached. That leads to a "freezing" of the parameters into the best match. The Doppler frequency can be taken directly from the optimized parameter set.

2.4.3 Gauss Modulated Cosine Function

Another possibility of a model-based frequency estimation is the use of the ACF. As the model ACF, the Gauss modulated cosine function

$$R_i^{(m)} = A_R G\left(\frac{\tau_i}{b_R}\right) \cos(2\pi \tau_i f_D) \tag{15}$$

with $\tau_i = i/f_s$ and the three parameters A_R, f_D and b_R can be used. Note that the ACF is symmetric about $\tau = 0$. For this reason there is neither a displacement of the Gauss envelope nor a phase in the argument of the cosine function. To reduce the number of iteratively optimized parameters the estimation of the Gauss envelope and the modulated cosine function are performed separately. To get a good pre-estimation of the Gauss envelope the ACF amplitude function H_i (equation 9) can be used. The appropriate model

$$H_i^{(m)} = A_R G\left(\frac{\tau_i}{b_R}\right) \tag{16}$$

with the amplitude A_R and the Gauss width b_R is used. To evaluate the deviation of the model from the original signal the error value

$$e = \sum_{i=1}^{N/2-1} \left(H_i - H_i^{(m)}\right)^2 \tag{17}$$

is used. The amplitude A_R can be expressed explicitly by

$$A_R = \frac{\sum_{i=1}^{N/2-1} H_i G\left(\frac{\tau_i}{b_R}\right)}{\sum_{i=1}^{N/2-1} \left(G\left(\frac{\tau_i}{b_R}\right)\right)^2}. \tag{18}$$

Note that the index runs only over half of the time lag range due to the symmetry and the value at $\tau = 0$ is ignored because of the noise.

The optimum of the parameter b_R has to be found iteratively starting with $b_R = N/(4f_s)$. The standard deviation of this parameter is $N/(4f_s)$ at the beginning and is reduced after 2 000 iteration steps to $1 \times 10^{-6}\,\mu$s. Only positive values should be tested. The reduced number of iteration steps compared to the PSD based estimation is sufficient because of the reduced parameter set to be optimized.

Once the optimum for the amplitude A_R and the width b_R of the Gauss envelope has been found the Doppler frequency can be estimated from the ACF with the reduced model

$$R_i^{(m)} = H_i^{(m)} \cos(2\pi\tau_i f_D) \tag{19}$$

using the fixed envelope function $H_i^{(m)}$. The error value is

$$e = \sum_{i=1}^{N/2-1} \left(R_i - R_i^{(m)}\right)^2 \tag{20}$$

and the searching procedure starts with $f_D = f_s/4$. The standard deviation of this parameter is $f_s/4$ at the beginning and is reduced after 2 000 steps to 1×10^{-6} MHz. The valid parameter range lies between f_c and $f_s/2$. The Doppler frequency can be taken directly from the optimized parameter set.

3. SIGNAL SIMULATION

The signal simulation gives an equidistant spaced sampled signal with $N = 256$ values and the sampling frequency $f_s = 10\,\text{MHz}$

$$u_i = A_t \left[G\left(\frac{t_i - t_0}{b_t}\right) \cos(2\pi t_i f_D + \phi) + \frac{G\left(\frac{t_i - t_0 - \delta_G}{b_t}\right) + G\left(\frac{t_i - t_0 + \delta_G}{b_t}\right)}{G\left(\frac{2\delta_G}{b_t}\right)} \right] + \tilde{u}_i \tag{21}$$

$$\tilde{u}_i = \tilde{g}\sqrt{\sigma_N^2} \qquad i = 0 \ \ldots \ N-1 \tag{22}$$

parameter	unit	mean m	variation range Δ
A	-	0.8	0.2
f_D	MHz	1.0	0.3
ϕ	-	1.1	3.0
t_0	μs	11.5	2.5
$\log_e \sigma_N^2$	-	-3	4
b_t	μs	2.0	0.5
δ_G	μs	1.3	0.25

Table 1: Mean values and variation range of burst simulation parameters

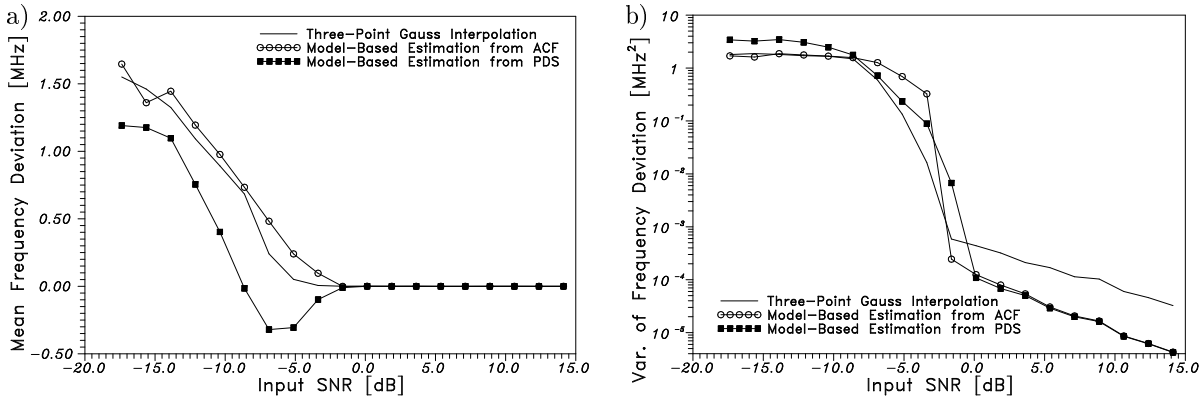

Figure 6: a) Mean frequency deviation and b) estimator's variances of frequency deviation

with the Gauss-like function $G(x) = e^{-x^2/2}$, the sampling times $t_i = i/f_s$, the signal amplitude A_t, the Doppler frequency f_D, the phase ϕ, the arrival time t_0, the noise component $\tilde{u}_i$, the noise power σ_N^2 and the Gauss distributed value $\tilde{g}$ with a variance of 1. The quantity b_t influences the width of the Gauss envelope. It corresponds to the size of the measurement volume. The quantity δ_G doesn't have a direct correspondence to a measurable quantity. It influences the modulation index of the simulated signal. Figure 1a shows one realization of a simulated burst signal using equations (21) and (22).

For each simulated burst signal all simulation parameters are changed. The parameter values are taken randomly from an interval $[m - \Delta; m + \Delta]$ with a constant distribution. For the variation of the noise power the logarithm $\log_e \sigma_N^2$ was used. In table 1 the mean values m and the variation range Δ of the simulation parameters are listed.

4. RESULTS

The signal simulation and the three frequency estimations have been carried out 10 000 times. In figure 6 the mean frequency deviation and the variances of the estimators are shown in comparison. In the stable range (above 0 dB) all estimators are unbiased. Both model-based methods have a much smaller estimation variance than the three-point Gauss interpolation. A significant difference between the model-based methods cannot be seen. Below 0 dB the PSD based estimates and below -2 dB the ACF based estimates and below -4 dB the three-point Gauss interpolation become unstable. The variances of the frequency estimates increase rapidly. For very small input SNRs the variances of all algorithms are constant with respect to the random frequency estimates taken from a limited interval.

5. CONCLUSIONS AND PERSPECTIVE

The results of the performance test show that the model-based estimation of the Doppler frequency from LDA burst signals is possible in principle. The results for the estimation based on the PSD and the estimation based on the ACF are very similar. That indicates that the parameter estimation for the Gauss envelope of the ACF and the modulated Doppler signal can be performed separately. That leads to a faster routine because the number of iteration steps to optimize two parameters at once has to be 10 times as large as for only one parameter because of the larger dimension of the parameter range.

Both model-based routines show however high probability of a completely wrong estimate. A possible way to overcome this is a pre-estimation of all model parameters with more stable algorithms in combination with a reduced searching interval.

The new Doppler frequency estimators take all values of the PSD/ACF into account. That leads to a very small random deviation of the estimates. On the other hand the new estimators require the entire PSD/ACF for a correct estimation. The start of the burst record should be long before any burst detection algorithm can give a signal.

One parameter of the investigated model, the Gauss width b_R, was not used. But it could improve the estimation of the transit time. So far the transit time is quantified by an integral number of Doppler periods and it is amplitude dependent. Defining the edges of the measurement volume to be the points with e^{-2} of the maximal amplitude, the transit time is $\mathrm{TT} = 4b_t = 2\sqrt{2}b_R$. This transit time estimator is more reliable, it has a smaller variablity, no quantization and it is amplitude independent.

The searching routines take too much time for online measurements (20 s for the ACF and 100 s for the PSD on a Pentium II system). In future, faster routines should be developed that work together with more stable pre-estimations.

Another future development could be to include non-Gaussian beam models with ACF models other than the Gauss modulated cosine function.

REFERENCES

[1] W K George and J L Lumley. The laser Doppler velocimeter and its application to the measurement of turbulence. *J. Fluid Mech.*, 60:321–362, 1973.

[2] K Hishida, K Kobashi, and M Maeda. Improvement of LDA/PDA using a digital signal processor (DSP). In *Proc. 3rd Int. Conf. on Laser Anemometry*, Swansea, UK, 1989.

[3] D Matovic and C Tropea. Estimation of LDA signal frequency using the autocovariance (ACF) lag ratio method. *J. Phys. E: Sci. Instrum.*, 22:631–637, 1989.

[4] D Matovic and C Tropea. Spectral peak interpolation with application to LDA signal processing. *Meas. Sci. Technol.*, 2:1100–1106, 1991.

[5] E Müller, H Nobach, and C Tropea. Model parameter estimation from non-equidistant sampled data sets at low data rates. *Meas. Sci. Technol.*, 9(3):435–441, 1998.

[6] D C Rife and R R Boorstyn. Single-tone parameter estimation from discrete-time observations. *IEEE Trans. Information Theory*, 20:591–598, 1994.

[7] C Tropea, G Dimaczek, J Kristensen, and C caspersen. Evaluation of the burst spectrum analyzer LDA signal processor. In *Proc. 4th Int. Symp. on Appl. of Laser Techn. to Fluid Mechanics*, Lisbon, Portugal, 1988. paper 2.22.

[8] H L van Trees. *Detection, Estimation and Modulation Theory: Part 1.* Wiley, New York, 1968.